CHAPTER 1

Diamondoid Hydrocarbons

Jacob Filik

Biophotonics Research Unit, Gloucester Royal Hospital, Great Western Road,
Gloucester, GL1 3NN, UK
Tel: 08454 22 5471
(*Previously at School of Chemistry, University of Bristol*)
Jacob.filik@gmail.com

J. Filik, "Diamondoid Hydrocarbons", Chapter 1, pp. 1-26, in: *Carbon Based Nanomaterials*, Materials Science Foundations (monograph series), **Vol. 65-66**, Eds. N. Ali, A. Öchsner and W. Ahmed, Trans Tech, Switzerland, 2010), ISBN: 0-87849-155-4.

Table of Contents

1. INTRODUCTION

The term diamondoid is used to describe hydrocarbon molecules that are totally or largely superimposable on the diamond lattice. The lower limit of this definition is set at adamantane ($C_{10}H_{16}$) to prevent the inclusion of cyclohexane and other simple alkanes [1].

The diamondoid (or diamond hydrocarbon) classification can be further separated *into two* groups: (I) diamondoids that are only partly superimposable on the diamond lattice (Fig. 1 (a,b)), and (II) diamondoids which are completely superimposable on the diamond lattice (Fig. 1 (c,d)). Molecules in the latter group that can only be formed by the face-fusing of adamantane units (sharing 6 carbon atoms per pair of adamantanes) are known as polymantanes (Fig. 1 (e,f,g,h)).

The polymantanes form a natural series, starting with the smallest molecules (adamantane, diamantane and triamantane), and finishing with an infinite diamond lattice. Between these two points lie micro- and nano-crystalline diamond, and the higher diamondoid molecules. Whereas diamond micro- and nano-crystals are readily formed by chemical vapor deposition (CVD) [2] and shock/explosion synthesis methods [3], higher diamondoids are far less accessible, found only in minute concentrations in petroleum [4].

Higher diamondoids are particularly interesting because they bridge the gap between hydrocarbon molecules and nano-sized diamond crystals. The isolation of the higher diamondoids permits the experimental study of the effects of cluster size on the properties of the diamond structure, from the bulk to the molecular limit. Currently, applications of the higher diamondoids are in an early stage, with many of the fundamental properties yet to be determined.

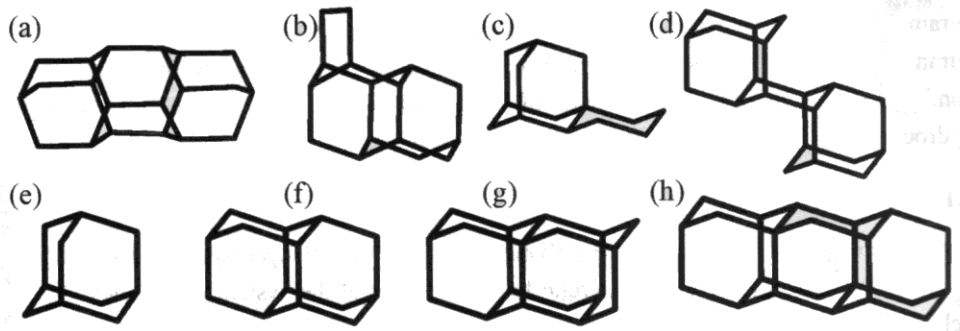

Fig. 1. Diamondoid hydrocarbons that are, (a,b) partly superimposable on the diamond lattice, (c,d) fully superimposable on the diamond lattice, and (e,f,g,h) polymantanes.

This chapter reviews the most important discoveries in the field of diamondoid hydrocarbons, starting with the synthesis and isolation of adamantane and ending with more recent advances.

2. AN INTRODUCTION TO DIAMONDOIDS

Tricyclo[3.3.1.1^{3,7}]decane (Fig. 1(e), using the systematic von Baeyer nomenclature, see section 2.1.1) was first isolated in 1933 from a sample of petroleum collected near the village of Hodonín in Moravia, part of what was then Czechoslovakia [5]. The name adamantane, derived from the Greek for diamond (adamas), was proposed on the basis of the X-ray structural analysis and the unusual physical properties of the material.

Bottger [6] completed the first synthesis of a functionalised adamantane cage in 1937, but it was Prelog and Seiwerth [7] who managed to remove the functional groups and produce pure adamantane, albeit in a low yield. Although this synthesis was improved over time, it was not until 20 years after the production of the first functionalised adamantane cage that a simple synthetic route to pure adamantane was discovered. This breakthrough was made by von Schleyer, and published in a single page communication in 1957 [8]. The synthesis was simple, involving two steps, and allowing substantial amounts of adamantane to be produced from a commercially available precursor.

The next polymantane in the series, pentacyclo[7.3.1.1^{2,1}.0^{2,7}.0^{4,11}]tetradecane (Fig. 2(f)), was the official emblem of the 1963 IUPAC congress in London, and was hence known as congressane. Cupas *et al.* [9] first synthesised this molecule in 1965, although it was isolated from petroleum a year later [10]. The name congressane was later replaced with the more systematic name, diamantane.

It was at this point that synthetic chemistry leapt ahead of the natural product isolation with the production of heptacyclo[7.7.1.^{13,15}.0^{1,12}.0^{2,7}.0^{4,13}.0^{4,11}] octadecane (Fig. 2(g), triamantane) in 1966 [11]. Despite this success, the synthesis of progressive polymantanes became increasingly difficult and it was another ten years before one of the four tetramantanes was prepared. In 1976 Burns *et al.* [12] successfully synthesised anti-tetramantane (Fig. 2(h)), so called because of its structural similarity to butane in its *anti* conformation. A more complete history of the synthesis of the diamondoids and other caged hydrocarbons can be found in reference [13].

2.1 SYSTEMATIC NOMENCLATURE

Two systems exist for naming the polymantanes; the von Baeyer system [14], which is traditionally used for naming polycyclic hydrocarbons and the system of Balaban and von Schleyer [1], which was specifically developed for the polymantanes.

2.1.1 THE VON BAEYER SYSTEM

The systematic von Baeyer nomenclature [14] is excellent for naming small cyclic systems, but it can rapidly become cumbersome when applied to larger polymantanes (see the von Baeyer name for triamantane above).

The von Baeyer name of a molecule is determined by the identification of the largest ring, the largest bridge across this main ring, and the lengths and positions of the other bridges in

the structure. The complete name indicates the number of rings (prefix), the lengths and positions of the bridges (numbers in parentheses) and the total number of skeletal atoms in the ring system (suffix).

As an example, let us consider how the name tricyclo[3.3.1.$1^{3,7}$]decane is derived for adamantane. The largest ring in the adamantane cage is 8 atoms long and has two single atom bridges across it (Fig. 2(a)). The adamantane cage has four bridgeheads (a bridgehead is any skeletal atom of the ring system which is bonded to three or more skeletal atoms), all of which are equivalent by symmetry. Two of these bridgeheads are selected as the main bridgeheads. The number of atoms in the chains between these two bridgeheads is recorded (two bridges of three carbons and one bridge of one carbon). A final bridge lies between atoms 3 and 7 on the main bridge and is a single carbon atom long (Fig. 2(b)). These figures give us the numbers displayed in the parenthesis at the centre of the name [3.3.1.$1^{3,7}$]. The prefix is obtained from the number of rings in the structure (equal to the minimum number of scissions required to convert the system into an open-chain compound), three in the case of adamantane (Fig. 2(c)). Finally, the ring system in adamantane contains ten carbon atoms giving us the suffix, decane.

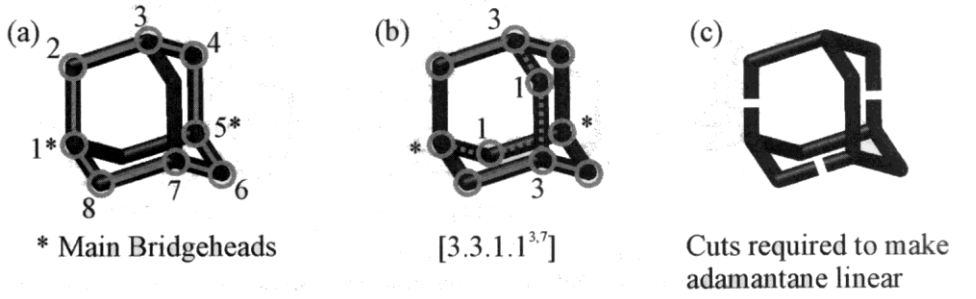

Fig. 2. Steps in the von Baeyer nomenclature (a) find the largest ring and label the main bridgeheads, (b) identify all the bridges across the main ring, and (c) determine the number of rings in the system.

2.1.2 THE BALABAN AND VON SCHLEYER SYSTEM

The von Baeyer nomenclature system is very flexible, but such flexibility is not required when naming regularly repeating structures like the polymantanes. Why is it necessary to label the bridges in every adamantane cage when you can just refer to the cage as a whole?

The trivial names adamantane, diamantane and triamantane are certainly a step towards a simplified naming system but these names are only possible because each of these molecules is a unique isomer made of one, two and three adamantane cages, respectively. Even the four tetramantane isomers are easily differentiated by trivial names (anti-, iso-, M and P skew-tetramantane) but the use of this kind of system becomes unfeasible when considering the 10

different pentamantanes or the hundreds of different octamantanes. Clearly, something more methodical is called for.

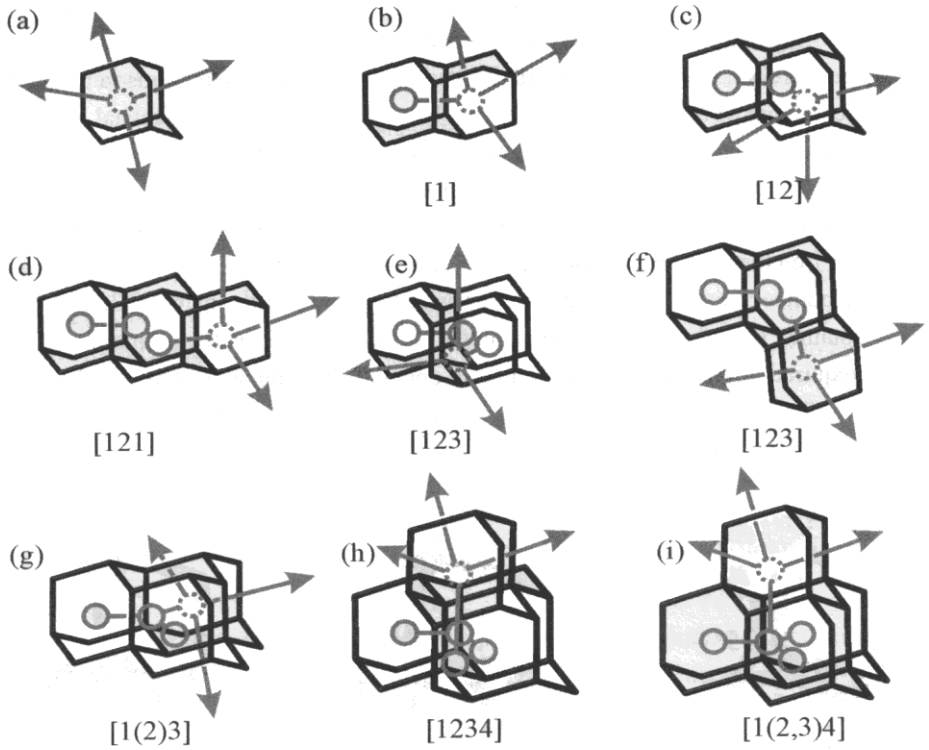

Fig. 3. Graphical representations of the Balaban and von Schleyer nomenclature for several daimondoid molecules.

In 1978, almost 20 years before the isolation of the higher diamondoid molecules, Balaban and von Schleyer [1] developed a naming system based on graph theory. Without delving into the terminology of graph theory, the basis of this idea is that adamantane has only four separate faces onto which other adamantane units can be fused to form polymantanes.

Starting with a single adamantane cage, there are four different directions in which a polymantane molecule could grow, as represented in Fig. 3(a). These directions are labelled with the numbers 1, 2, 3 and 4. Fusing together two adamantane units produces diamantane, which can be symbolised by a single line between the centres of the two adamantane units. In this new nomenclature, diamantane would be given the prefix '[1]', if it were not a unique isomer. The prefix number represents the orientation of the added adamantane unit with respect to the first adamantane (Fig. 3(b)). The number 1 is chosen out of the 4 directions simply because it is the lowest. The addition of a further adamantane unit to form

triamantane cannot happen in the 1 direction, because there are no empty faces remaining in this direction. All the remaining sites for addition are equivalent by symmetry, so the prefix '[12]' would be used for triamantane, had it also not been a unique isomer. In Fig. 3(c), the two lines connected at 109° through triamantane represent this addition. The first line represents the formation of diamantane (the [1…] in the prefix), the second line describes the fusing of another adamantane unit to diamantane to form triamantane (the [...2] in the prefix). Again the 1 and 2 directions are chosen because they have the lowest numerical value.

So far, only unique isomers have been produced, but the addition of another adamantane unit to triamantane can happen in four different ways. First, let us look at the case that would form anti-tetramantane. To produce this molecule, an adamantane unit is added to triamantane in the 1 position, *i.e.* in the same direction as that which produced diamantane from adamantane (Fig 3(d)). This produces the prefix [121] and thus anti-tetramantane becomes [121] tetramantane. If instead, an adamantane unit is fused to either of the remaining orientations on the terminal adamantane, the two enantiomers of skew-tetramantane, or [123] tetramantane are produced (Fig. 3(e and f)). To produce the final tetramantane isomer, an adamantane unit is fused to the central unit in triamantane. But this has caused a problem; until now what had always been a straight line connecting adamantane units has become branched (Fig 3(g)). Let us imagine walking through this molecule, starting by heading in the 1 direction, the path then splits into the 2 and 3 directions. In this naming system, a number in parenthesis is added to the prefix to represent branching, hence iso-tetramantane becomes [1(2)3] tetramantane.

Moving up to the pentamantanes, there are now many isomers that are easily recognisable by their respective prefix. A few examples are; [1212] pentamantane, formed by addition of an adamantane unit to the end of [121] tetramantane, [1234] pentamantane (Fig 3(h)), formed by the addition of an adamantane unit to [123] tetramantane, and [1(2,3)4] pentamantane, a tetrahedron of adamantanes (Fig. 3(i)).

The rules above are too concise to allow the naming of unknown polymantanes, but detailed enough to permit the determination of the correct molecular structure from a given prefix.

3. HIGHER DIAMONDOIDS IN OIL

By the mid-nineties, several polymantane structures had been discovered in petroleum by gas chromatography/mass spectrometry (GC-MS). First to be observed was triamantane in 1992 [15], tentatively followed by a whole selection of tetramantanes, pentamantanes and hexamantanes in 1995 [16].

The concentration of diamondoid molecules in crude oil ranges from 1-100 ppm, the most abundant structures being substituted and unsubstituted adamantanes and diamantanes [17]. The mechanism that leads to the formation of the diamondoids in oil wells is, as of yet,

unknown but Wei *et al.* [18] have recently shown that diamondoids can be produced by pyrolysis of kerogen on naturally occurring minerals.

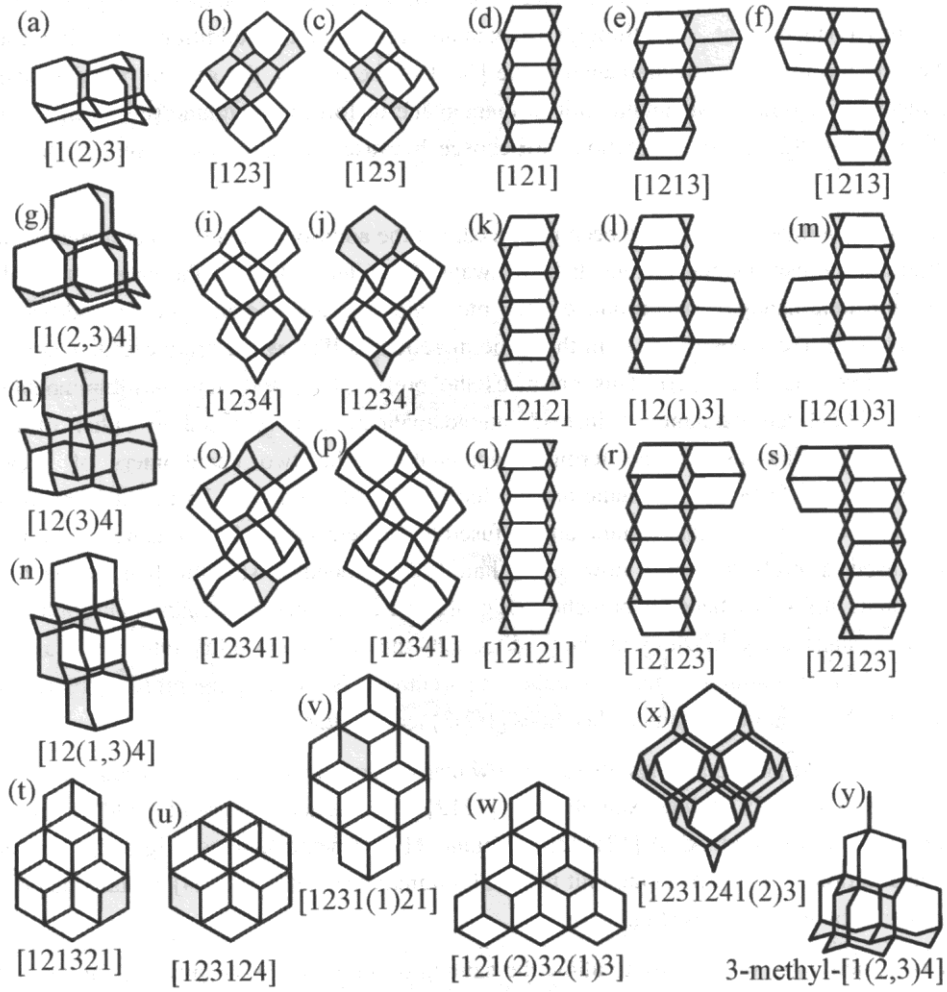

Fig. 4. Diamondoids isolated in Ref. [4]; tetramantanes (a,b,c,d), pentamantanes (e,f,g,h,I,j,k,l,m), hexamantanes (n,o,p,q,r,s), heptamantanes (t,u), octamantane (v), nonamantane (w), decamantane (x), and the alkylated pentamantane (y).

Large diamond crystals are known to be slightly thermodynamically unstable with respect to graphite, but this is not necessarily the case for sub-nanometre-sized clusters. Badziag *et al.* [19] have calculated that small hydrogen-terminated diamonds (~ 3 nm in size) are as stable as polycyclic precursors to graphite of the same hydrogen/carbon ratio. Further to this, at higher H/C ratios the tetrahedrally-bonded structures are more stable than hexagonally-bonded structures of a similar size. Therefore, the formation of diamondoids from petroleum

precursors is likely to be thermodynamically favoured, possibly helping to explain their existence.

The strong diamond backbone structure of the diamondoids gives them a high thermal stability compared with other crude oil components. Dahl *et al.* [17] exploited this fact by measuring the concentration of specific diamondoids (methyldiamantanes) to measure the extent of cracking (thermal breakdown of heavy hydrocarbons to smaller ones) in oil wells and hence estimate the extent of oil destruction. During this study it was also observed that, at certain sites, diamondoid hydrocarbons were at such high concentrations that they crystallized during the production process to cause plugging problems in the wells [17].

3.1 ISOLATION OF THE HIGHER DIAMONDOIDS

In 2003 Dahl *et al.* published an article in the journal Science [4] announcing the isolation and crystallisation of a large selection of higher diamondoids from petroleum. This selection contained a range of sizes and geometries from the simple linear [121] tetramantane, though screw-shaped chiral pentamantanes, to the "adamantane of adamantanes" [1231241(2)3] decamantane. In total, all four tetramantanes, nine pentamantanes, one hexamantane, two heptamantanes, two octamantanes, one nonamantane, one decamantane, and one undecamantane were isolated (see Fig. 4).

The diamondoids were obtained from condensates produced at the Norphlet Formation, Gulf of Mexico. The higher diamondoid fractions were obtained by vacuum distillation, followed by pyrolysis to remove non-diamondoid fractions, ending with several chromatographic steps and recystallisation from acetone [4]. Single crystal X-ray diffraction was used on a selection of purified diamondoid samples to determine the orientation and packing of the molecules in the crystals.

3.2 [12312] HEXAMANTANE (CYCLOHEXAMANTANE)

Soon after the isolation of the higher diamondoids, a detailed verification of the structure of the disc-shaped diamondoid, [12312] hexamantane was published [20]. This study displayed the first NMR (both ^{13}C and ^{1}H) and Raman spectra ever taken of a higher diamondoid molecule.

The ^{1}H-decoupled ^{13}C NMR spectrum displayed three sharp lines at shifts of 37.81, 38.51 and 47.34 ppm. In the ^{13}C DEPT NMR spectrum the 38.51 ppm signal adopted a negative phase, indicating that the carbon atoms which produced this signal were bonded to an even number of H atoms (in this case two). The other two lines are due to methine carbons (a carbon with four single bonds, where one bond is to hydrogen) in different environments. The signal from the two equivalent quaternary carbon atoms was absent, possibly due to the small amount of sample used and the expected long longitudinal relaxation times [20].

The Raman spectrum of [12312] hexamantane was found to contain a large number of peaks with positions ranging from 300–2920 cm^{-1}. Tentative assignments of these peaks were

made by comparison with the Raman spectra of adamantane, nano-phase diamond and bulk diamond. A fuller discussion of the Raman spectra of the higher diamondoids, including [12312] hexamantane, can be found in section 4.2.1.

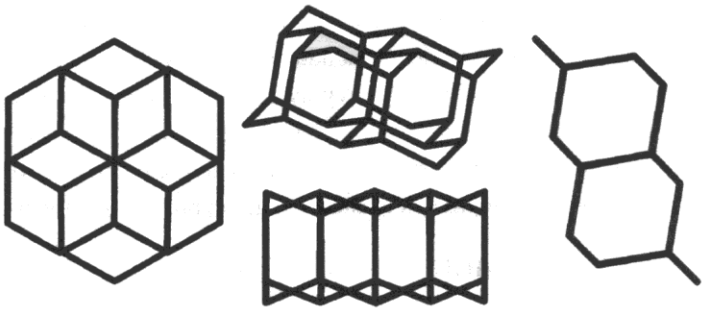

Fig. 5. Various orientations of [12312] hexamantane.

4. PROPERTIES OF THE DIAMONDOIDS

The properties of the higher diamondoids, especially their relationship to the properties of bulk diamond, were of great scientific interest even before the isolation of these exciting structures. Over ten years prior to the isolation of higher diamondoids, Shen *et al.* [21] determined their carbon-carbon bond lengths, total energies and heats of formation, using various semi-empirical and *ab initio* methods.

Since the higher diamondoids have only been available for such a short period of time (less than five years), many of the proposed applications are based on extrapolating the current uses of the lower diamondoids.

4.1 CURRENT APPLICATIONS OF THE LOWER DIAMONDOIDS

By far the most successful application of the lower diamondoids is in the pharmaceutical industry. Amantadine (1-aminoadamantane, Fig 6 (a)) and rimantadine (1-(1-adamantyl) ethanamine, Fig 6 (b)) are both used to relieve and prevent the symptoms of influenza A in adults [22]. Amantadine has also been shown to delay the onset of dementia in patients with Parkinson's disease [23]. Another adamantane derivative, memantine (1-amino-3,5-dimethyl-adamantane, Fig 6 (c)) is used to reduce the symptoms of Alzheimer's disease [24]. Adamantane is also at the heart of a new anti-malarial drug called OZ277 [25], where the adamantane cage is used to protect the active secondary ozonide group.

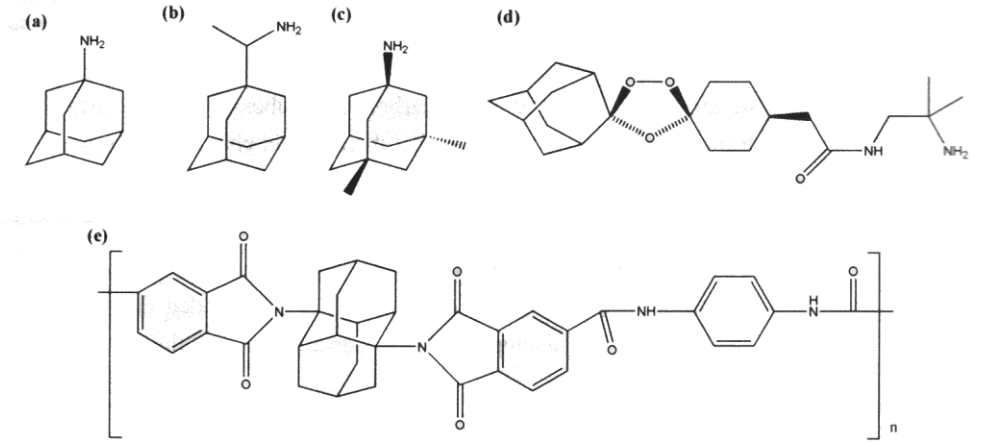

Fig. 6. Structures of (a) amantadine, (b) rimantadine, (c) memantine, (d) OZ277 and (e) the high thermal stability polymer in [28].

The high strength and thermal stability of the diamond structure suggests that the diamondoids could be used to produce excellent engineering materials. The most obvious way of converting the individual molecules into novel materials is by polymerisation. Several polymers of both adamantane [26,27] and diamantane [28] (Fig 6 (d)) have been produced which show high thermal stability (stable up to 400°C) and good mechanical properties (tensile strengths ranging from 35.5 - 46.9 MPa). Adamantane has also been used in light emitting polymers to break up the π-conjugation and prevent interchain interactions [29,30].

4.2 FUTURE APPLICATIONS OF THE HIGHER DIAMONDOIDS

Considering the impact the lower diamondoids have made in pharmaceutical and polymer research it is very likely that the higher diamondoids will find applications in these areas also. Since the higher diamondoids are larger structures, and hence slightly closer to diamond, there are many more proposed uses for these molecules which are yet to be investigated.

One possible area that the unique structure and size of the higher diamondoids maybe useful is in the growth of chemical vapour deposition (CVD) diamond. To grow diamond on a non-diamond substrate, the substrate must be processed to increase the density of growth sites [31]. Traditionally substrates have been abraded (often ultrasonically) with nanocrystalline diamond powder [32] prior to plasma deposition, or a bias enhanced nucleation step [31] is utilized, to aid the nucleation of diamond crystals. The small size and

perfect uniformity of the higher diamondoids (relative to nanodiamond powders) have led to suggestions that these structures could be an excellent seed material for CVD diamond growth [4].

As well as possibly supplanting nanodiamond from its current uses, the higher diamondoids may also eventually compete with carbon nanotubes in certain areas. A theoretical study by McIntosh *et al.* [33] has shown that diamondoid chains could potentially rival carbon nanotubes as low-voltage electron emitters for flat panel displays.

Having the same strong and inert structure as diamond one of the more futuristic applications of the higher diamondoids is in carbon-based nanomachines. These technologies are certainly a long way off but a molecular computer aided design (CAD) program for designing diamondoid-based nanotechnology has already been developed [34].

4.3 VIBRATIONAL SPECTROSCOPY

The vibrational spectrum of adamantane has been studied both experimentally and theoretically since as early as the 1970's [35]. These studies used valence force fields to assist in the assignment of spectral lines, but as time and computing power have progressed, assignment with more advanced *density functional* methods has become commonplace. This ability to calculate the vibrational frequencies and infrared/Raman intensities with precision and relative simplicity has led to spectra being calculated for large diamondoid structures as an approximation to the spectra of diamond surfaces [36] or nanodiamond clusters [37].

4.3.1 RAMAN SPECTROSCOPY OF DIAMONDOIDS

The most commonly used spectroscopic method to analyse diamondoid molecules is Raman spectroscopy. There are many studies of adamantane and its derivatives using Raman spectroscopy. Good examples include work on adamantane and perdeuterated adamantane [38,39], 1,1′-biadamantane [40] and 2-adamantanone [41], perfluoroadamantane [42] and amantadine [43] (including surface-enhanced Raman).

Before the isolation of the higher diamondoids [4] publications studying the Raman spectra of diamondoids larger than adamantane were rare. The Raman spectra of adamantane, diamantane and triamantane were studied in 1980 by Jenkins and Lewis [44]. They focused on the variation of the low frequency lattice modes with temperature, to determine the crystal phase changes.

As mentioned above, the first higher diamondoid studied by Raman spectroscopy was [12312] hexamantane. In the original paper by Dahl *et al.* [20], the spectral lines were only approximately assigned by comparison with spectra of similar structures. Richardson *et al.* [45] produced a fuller assignment of the Raman spectrum of this molecule. They used density functional theory (DFT, specifically the Perdew–Burke–Ernzerhof generalized-gradient approximation) and a large basis set (a total of 1480 basis functions) to calculate the vibrational frequencies and Raman/IR intensities of this molecule. These were then used to

confirm that the Raman spectrum obtained by Dahl *et al.* [20] was definitely from [12312] hexamantane.

The first article that included a large selection of diamondoid Raman spectra was produced by Filik *et al.* [46] in 2006. This study included experimental and calculated Raman spectra of a broad selection of diamondoid molecules ranging from adamantane to [121321] heptamantane. Each diamondoid was shown to produce a unique Raman spectrum, making differentiation between the molecules rather simple.

One of the more interesting features of the diamondoid Raman spectra is the position of the cage-breathing modes when compared to the structure of the molecule. The breathing modes tend to produce the highest intensity Raman signals in the region of the spectra below 800 cm^{-1}. The highest frequency cage-breathing mode is observed in the spectrum of the smallest diamondoid, adamantane (Fig. 7(a)), which only has a single breathing mode, (757 cm^{-1}) due to its T_d point group. Larger diamondoids can have multiple breathing modes depending on the symmetry of their molecular structure; the frequencies of these modes are correlated with the dimensions of the molecule. For example, the spectra of diamantane (Fig. 7(b)), triamantane (Fig. 7(c)), all three tetramantanes and all of the pentamantanes studied, with the exception of [1(2,3)4] pentamantane (Fig. 7(e)), all have a breathing mode

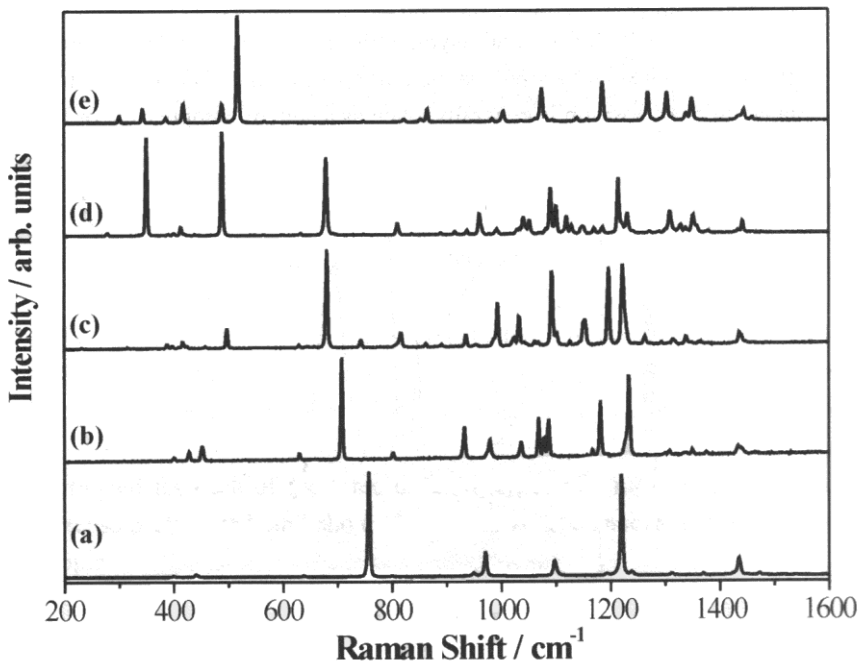

Fig. 7. Raman spectra of diamondoids (a) adamantane, (b) diamantane, (c) triamantane, (d) [121] tetramantane and (e) [1(2,3)4] pentamantane [42].

around 680 cm^{-1}. The breathing motions that occur around this wavenumber are all motions of structures that are only one adamantane unit wide. [1(2,3)4] pentamantane does not display a breathing mode near this frequency because it is the smallest diamondoid to have no parts of its structure that are only one adamantane unit wide. It is a solid tetrahedron of adamantane units. This is a small indication of how diagnostic the breathing modes in the Raman spectra of the diamondoids can be. Further examples can be found in reference [46].

4.3.2 COMPARISON OF DIAMONDOID RAMAN SPECTRA TO THAT OF NANOCRYSTALLINE DIAMOND

The technique of Raman spectroscopy is excellent for the analysis of carbon-based materials, from diamond [47] to diamondoids [46], graphite [48] to nanotubes [49] and even amorphous carbon [50]. Despite its flexibility, a major problem with Raman spectroscopy is the difficulty in assigning unexpected signals in spectra of new materials. A fine example of this problem is the application of Raman spectroscopy to nanocrystalline diamond.

When dealing with large perfect crystals, where the lattice size is effectively infinite, only certain phonons are Raman active, and the Raman spectra contain very few peaks. In nanocrystalline or highly disordered samples, the selection rules break down, allowing more vibrational modes to become Raman active. The effects of this appear in two ways: (a) shifting and asymmetric broadening of existing peaks and (b) the appearance of new signals activated by disorder. The activation of the D peak with disorder in graphite [48] is an example of the latter. Peak shifting and asymmetric broadening has been observed in the 1332 cm^{-1} signal of shock-synthesised nanodiamond powders [51], but in diamond thin films any change in peak position is generally taken as a sign of compressive or tensile stress in the film [52].

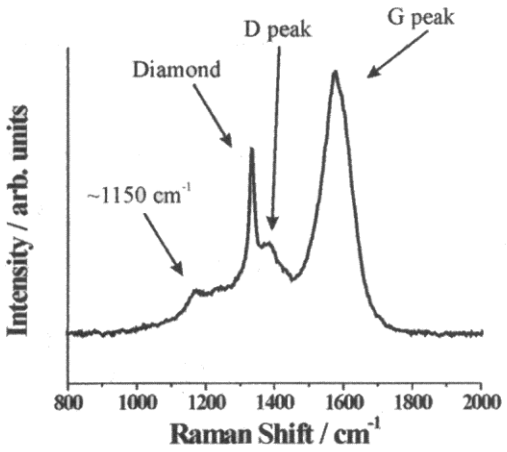

Fig. 8. Raman spectrum of nanocrystalline diamond taken with 325 nm excitation. The sample was deposited by microwave CVD at 0.8 kW and 100 Torr, from a gas mixture containing 97% Ar, 2% H_2 and 1% CH_4.

The appearance of new signals activated by disorder in CVD nanodiamond films is still a subject of some controversy. Figure 8 shows a 325 nm Raman spectrum of a film grown under typical nanodiamond conditions. The diamond line and the G and D peaks are present, but there is also a small, broad signal at ~1150 cm^{-1} which is not observed in the spectrum of microcrystalline diamond. The presence of this peak is often taken as direct evidence for nanosized diamond crystals, since, at first it, was thought that it was a disorder-activated peak [53]. It is now believed that this peak arises from sp^2-hybridised structures, such as polyacetylene-like molecules, that may be present on the surface and in grain boundaries [54-56].

The interpretation of the Raman spectra obtained from nanocrystalline diamond powders is also not without controversy. A broad, weak signal has been observed at ~ 600 cm^{-1} in the Raman spectrum of sub-200 nm diamond particles [51,57]. The intensity of this signal has been shown to be inversely proportional to the size of the particles investigated [51], a trend which might be expected for a peak activated by particle size effects. So far, this peak has only tentatively been assigned as longitudinal acoustic phonons near the Brillouin zone boundary. The theory behind this assignment is the close proximity of this signal to a maximum in the diamond vibrational density of states (VDOS).

However, instead of considering the confinement of the diamond lattice, several studies have compared peaks observed in the experimental and theoretical Raman spectra of diamondoids to these unassigned nanodiamond peaks, in the hope of discovering their chemical origin.

The first study to compare the signals seen in the Raman spectra of nanophase diamond to those seen in the diamondoid spectra was performed by May *et al.* [58] in 1998. Only the Raman spectra of the two smallest diamondoids, adamantane and diamantane, were used in this study, and although the spectra of both these molecules had peaks that correlated with the nanophase diamond signals, the authors concluded that they are unlikely to be the source of the signal.

More recently, Zhang *et al.* [59] conducted a purely theortical study to assign these nanophase diamond modes. They used DFT to calculate the Raman spectra of a selection of diamondoids, polyaromatic hydrocarbons and polyacetylene chains. These molecules were selected as being good approximations of nanodiamond, nanographite and polyacetylene; the main structures expected to be found in CVD nanodiamond films. Comparing the average spectra determined for each of the three different types of structure, they deduced that a relatively intense peak at 480 cm^{-1} should be indicative of a nanocrystalline diamond phase within a sample.

The validity of this result was questioned soon after in an article by Filik *et al.* [37]. In earlier work [46], it was observed that the diamondoid cage-breathing modes tend to produce the highest intensity Raman signals in the region of the spectra below 800 cm^{-1}, and that the frequencies of these modes were strongly dependant on the dimensions of the diamondoid structures. For the size of diamondoids studied by Zhang *et al.* (up to $C_{44}H_{42}$), a strong peak at 480 cm^{-1} would have to be related to the cage-breathing modes. Since the breathing modes frequencies are size dependant, it is unlikely that the breathing mode frequency of a > 1 nm diamond crystal would be near to that of a < 1 nm diamondoid molecule. Hartree-Fock calculations of a ~ 1 nm diamondoid molecule ($C_{84}H_{64}$) by Filik *et al.* [37] showed that there should, in fact, be no relatively strong Raman modes in the region 400–1000 cm^{-1} assignable to the diamond structure (Fig. 9(a)), and that this gap should widen as the diamondoid structure becomes larger.

Performing further calculations (different basis sets, on different sized diamondoids (Fig. 9(b)), including the addition of artificially heavy hydrogen atom termination (Fig. 9(c)) to approximate the confinement of diamondoid structures within a film) led the authors to suggest that the broadened ~ 1332 cm^{-1} bulk diamond line and the breathing modes (which for a ~ 3 nm diamond nanocrystal should be lower than 200 cm^{-1}) should be the only Raman signals produced by nanosized diamond crystals. They concluded that any features in the Raman spectra of nanocrystalline diamond samples that resembled peaks in the diamond VDOS must be due to defects, surface structures, amorphous material, or any other nondiamond material in the sample, and cannot be used as definitive evidence for nanocrystalline diamond within a sample [37].

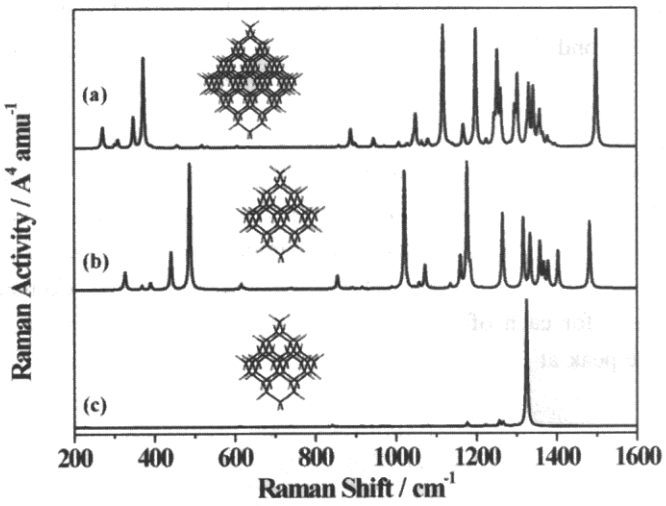

Fig. 9. Theoretical Raman spectra of large diamondoid molecules (a) $C_{84}H_{64}$ HF/3-21G H_{mass} = 1 amu, (b) $C_{35}H_{36}$ HF/6-31+G H_{mass} = 1 amu, and (c) $C_{35}H_{36}$ HF/6-31+G* H_{mass} = 100 amu [33].*

4.3.3 INFRARED (IR) ABSORPTION SPECTROSCOPY

The analysis of diamondoids by IR absorption spectroscopy is generally done either as a complement or as an alternative to Raman spectroscopy. Many of the Raman studies on adamantane and its derivatives already mentioned, also included the assignments of the IR absorption spectra [34,35,37]. IR absorption spectroscopy has also been used to study the phase changes in the adamantane crystal with temperature [60].

The vibrational frequencies and IR absorption intensities of a selection of C_{3v} symmetry diamondoids were produced by Chen *et al.* [36] as a model of the spectrum of a diamond C(111) 1×1 surface. The aim of this investigation was to explain the reduction in intensity and disappearance of the diamond C(111)-1×1 surface CH stretch mode at 2834 cm^{-1} for diamond particles with diameters below 100 nm. Their study provided *ab initio* evidence for the hypothesis that the <111>-type facets on diamond crystallites of diameter < 25 nm are too small to produce the commonly observed, well-defined, surface CH stretching features. These CH stretching features are important for confirming the existence of nanodiamond crystallites in the circumstellar medium from IR emission spectra [61].

Before experimental IR absorption spectra of the higher diamondoids had been produced, Lu *et al.* [62] calculated some of the vibrational frequencies and IR intensities using DFT and the B3LYP/6-31(d) basis set. They used these frequencies to determine the VDOS and local vibrational density of states (LVDOS) of [1231241(2)3] decamantane. Comparison of the LVDOS of the inner-most shell of carbon atoms in [1231241(2)3] decamantane with the VDOS of diamond, led the authors to suggest that the inner carbon atoms in higher diamondoids may exhibit local vibrational properties similar to those of bulk diamond.

Oomens *et al.* [63] published the first experimental IR absorption spectra of higher diamondoids in 2006 (Fig. 10). The spectra were compared to vibrational frequencies and IR intensities determined using B3LYP/D96(d,p). It was observed that the spectra of the diamondoids could all be split into four common regions: (I) CH stretch at ~ 2900 cm^{-1}, (II) CH_2 scissor at 1450 cm^{-1}, (III) CH_2 rock, wag, and twist with some CC stretch from 1400-1000 cm^{-1} and (IV) skeletal deformations < 1000 cm^{-1}. The calculated frequencies showed reasonable agreement with the experimental values, but the intensities, especially of the modes in (III) and (IV), were severely underestimated, no matter what sized basis set was used in the calculations. Several possible causes were proposed for this discrepancy, including shortcomings in the theory and the interaction of the molecules with their solid environment. Nevertheless, the authors concluded that the IR absorption spectra provided a fingerprint for this class of molecule, which could be useful in many areas, especially the detection of diamondoid-like material in different astrophysical objects.

4.4 ELECTRONIC STRUCTURE

The relationship between the electronic structure of the diamondoids, nanocrystalline diamond, and bulk diamond is particularly interesting.

For nanocrystals of silicon and germanium, reduction of the crystal size from ~ 5 nm to ~ 1 nm has been shown to produce a well-defined increase in the band gap energy, which correlates well with theory [64,65]. Experiments on diamond nanocrystals, on the other hand, have not yielded such clear-cut results.

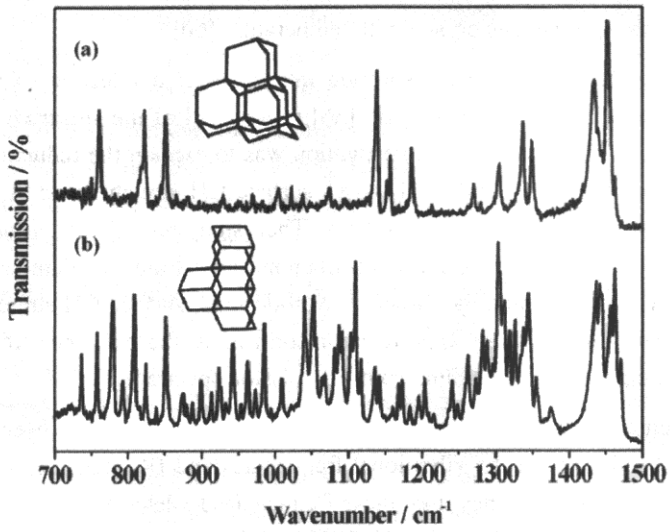

Fig. 10. ATR FT-IR spectra of (a) [1(2,3)4] pentamantane, and (b) [12(1)3] pentamantane [59].

Chang *et al.* [66] have studied a series of nanodiamond thin films by X-ray absorption spectroscopy (XAS). The diamond films were grown by microwave plasma enhanced CVD. The mean diamond grain size of each film was determined from transmission electron microscopy dark field images, and ranged from 3.5 nm to 5 μm, depending on the deposition conditions. Analysis of the carbon K-edge X-ray absorption near edge structure (XANES) spectra of the diamond films suggested that widening of the energy gap by quantum size effects was observable for comparatively large diamond crystallites (~ 18 nm), but these results remain controversial [67,68].

Raty *et al.* [69] used X-ray absorption spectroscopy, x-ray emission spectroscopy and *ab initio* calculations to study the band gaps of explosion-synthesised nanodiamonds. The results of their calculations showed that quantum confinement had no appreciable effect on the optical gap of diamond clusters for diameter larger than 1 nm. Comparison of the X-ray absorption and emission spectra of a 4 nm diamond particle with that of bulk diamond was consistent with the results of the calculations, showing no blue-shift in the position of the conduction and valence band edges.

These results were clearly at odds with the observations of Chang *et al.* [66], whose results suggested that a large change should be seen for such a small crystallite. Raty *et al.* proposed that the poor quality and high graphitic/amorphous carbon content of the nanodiamond films

used by Cheng *et al.* may have led to the observed deviation of their nanodiamond spectra from that of bulk diamond.

Prior to the publication of data on the electronic structure of higher diamondoids, several groups had used *ab initio* calculations to determine these properties.

In 2004 McIntosh *et al.* [33] produced a theoretical study on the use of diamondoids as functional nanostructures. Their article included investigations into the electronic structure of isolated diamondoids, dative bonding between diamondoids doped with boron and nitrogen, and interactions between diamondoids and carbon nanotubes. The energy difference between the highest occupied molecular orbital and lowest unoccupied molecular orbital (HOMO-LUMO) calculated in this study were found to show a similar variation with molecular size as the band gap calculation of Raty *et al.* [69], mentioned above.

Further work by Drummond *et al.* [70] and Lu *et al.* [71] also studied the electronic structure of the diamondoids by using theoretical methods. The findings of both these articles confirmed the hypothesis that quantum confinement effects disappear in diamond crystals larger than ~ 1 nm.

The first experimental studies of the electronic structures of diamondoid molecules were performed by Willey *et al.* [72] in 2005. These experiments measured the X-ray absorption of perfect, free, neutral diamondoids of various sizes between adamantane and [12312] hexamantane. The diamondoid C K-edge absorption spectra were found to exhibit sharp features ~ 2.3 eV below the absorption onset of a bulk diamond reference sample, which correlated with the structure of the diamondoid hydrogen surface termination. Despite this major difference, the spectra of the larger diamondoids were found to show some of the basic features of the band structure of bulk diamond (e.g. the second absolute gap at 303 eV). At higher energies, the pre-edge features merge into a broad resonance centred at 292 eV. This feature was attributed to the σ^* states of the C-C bonds of the diamondoid interior, that is, the bulk-diamond-like states. No shift in absorption onset with increasing size was observed in either the surface C-H or bulk C-C states, as would be expected in the quantum confinement model. Instead, it was concluded that the hydrogen surface atoms have a large impact on the diamondoid electronic structure, by dominating the lowest unoccupied states and hence a more molecular model is required to describe the ultimate size limit of diamond crystals.

A year later, Willey *et al.* [73] followed up this article with a larger study, this time using X-ray absorption and soft X-ray emission spectroscopy to investigate the both the LUMO and HOMO states of solid diamondoid powders. The X-ray absorption spectra were found to be very similar to those obtained from the gas phase molecules, although without some of the fine structure. Again, no shift in absorption onset with increasing diamondoid size was found. On analysing the emission spectra, a downshift in the position of HOMO states with decreasing diamondoid size became apparent. Since there was no shift in the LUMO, the positions of the HOMO states were used to estimate the band gap of the diamondoids. These

estimated values were then compared to the calculated values of McIntosh *et al.* [33], Drummond *et al.* [70] and Lu *et al.* [71]. The quantum Monte Carlo calculations of Drummond *et al.* [70] were found to provide the best fit between the experiment and theory, producing the best prediction of the relative change in gap energy. The evidence from these experiments suggest that there is an increase in the band gap with decreasing cluster size, hence there is quantum confinement but it only occurs in the occupied states.

4.5 REACTIVITY

Some of the most promising applications of the higher diamondoids, i.e. advanced polymers and pharmaceuticals, rely on the ability to functionalise the surfaces of these molecules. Site-selective functionalisation of this sort of molecule is a challenging task due to the similarly reactive tertiary C-H bonds and the lower reactivity of, and steric hindrance around, secondary carbon atoms [74].

As an assessment of the reactivity of the higher diamondoids, Fokin *et al.* [74] compared the experimental functionalisation of diamantane with different reactants, to the computed structures of the radicals, cations, and radical cations of a selection of higher diamondoids. The aim of their study was to determine which synthetic approaches/reagents were most effective at discriminating between the non-equivalent, yet similarly reactive tertiary carbon positions. In the reactions with diamantane, which has two non-equivalent tertiary carbon sites, it was observed that opposite selectivities could be obtained by using electrophiles (for the 1- position) and outer-sphere single electron transfer (SET) oxidizers (for the 4-position). The SET oxidizer selectivity matched the results of the diamantane radical cation computations, which showed elongation of the C^4-H bond, relative to the other C-H bonds.

This work was extended by Schreiner *et al.* [75], who studied the selective functionalisation of triamantane and [121] tetramantane. They found that, in both cases, photoacetylation with triplet diacetyl led to substitution at the apical positions with high selectivity. Reaction in the presence of electrophiles gave mixtures of all possible tertiary substitution products

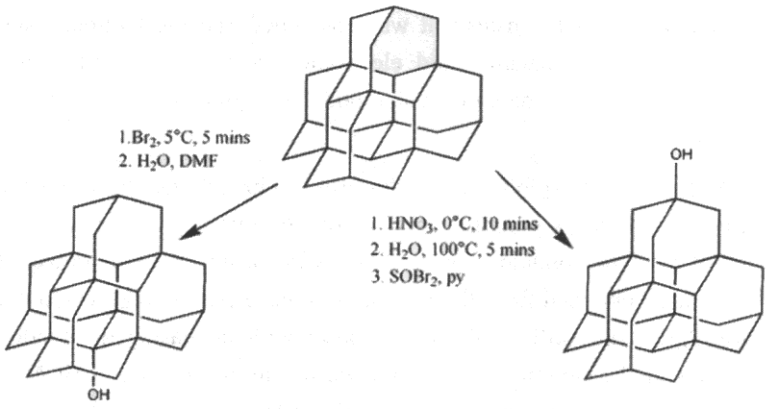

Fig. 11. Site-specific hydroxylation of [1(2,3)4] pentamantane at different tertiary carbons [74].

for triamantane, but only medial substitution products in high yields for [121] tetramantane. In total, more than 20 mono- and difunctionalised diamondoids were reported in this study, making a large step towards the use of higher diamondoids as building blocks for nanotechnology. Tkachenko *et al.* [76] used the method of Schreiner *et al.* [75] to produced diamondoid alcohols, which they then thiolated by reaction with thiourea. Thiolation permits the attachment of the diamondoids to noble metal surfaces to form self-assembled monolayers (SAMs).

[1(2,3)4] pentamantane (Fig. 11), the diamondoid tetrahedron, is the largest of the higher diamondoids to be functionalised [77]. Again it was observed that despite the similar reactivities of the diamondoid C-H bonds, selective functionalisation was relatively simple, and that the selectivity of the functionalisations increased with increasing diamondoid order. Reaction of [1(2,3)4] pentamantane with neat bromine produced mono- and di-bromination at the most sterically hindered positions on the molecule (2 and 2,4 positions), suggesting the reaction was kinetically controlled. Nitration of the molecule produced mono- and di-substitutions at the apical positions, although the mononitrate could not be isolated, as it was hydrolytically unstable and immediately converted to the alcohol (Fig. 11). It was then shown that the apical alcohol could be further converted to a thiol using the scheme of Tkachenko *et al.* [76].

5. CONCLUSIONS

The four years since the isolation of the higher diamondoids have seen a significant expansion in the research of these exciting structures. The availability of these molecules has greatly impacted many areas; ranging from the identification of nanodiamond by Raman spectroscopy, through the assignment of astronomical IR emission spectra, to the confirmation of theoretical predictions on quantum confinement in diamond.

The surprising ease of selective functionalisation of the diamondoids, especially thiolation, is the first step in the creation of many novel diamondoid-based chemicals and materials. Whether in high strength, high temperature polymers, self-assembled monolayers or pharmaceuticals, it is clearly just a matter of time before the stability, stiffness and extraordinary range of geometries (including chiral structures) allow the true potential of the higher diamondoids to be realised and exploited commercially.

REFERENCES

[1] A.T. Balaban and P. von R. Schleyer: Tetrahedron Vol. 34 (1978), pp. 3599ff.

[2] M. N. R. Ashfold, P. W. May, C. A. Rego, and N. M. Everitt: Chem. Soc. Rev. Vol. 23 (1994), pp. 21ff.

[3] N. Greiner, D. Phillips, J. Johnson, and F. Volk: Nature Vol. 333 (1988), pp. 440ff.

[4] J. E. Dahl, S. G. Liu, R. M. K. Carlson: Science Vol. 299 (2003), pp. 96ff.

[5] S. Landa and V. Machacek: Collect. Czech. Chem. Commun. Vol. 5 (1933), pp. 1ff.

[6] D. Bottger: Chem. Ber. Vol. 10 (1937), pp. 314ff.

[7] V. Prelog and R. Seiwerth: Chem. Ber. Vol. 74 (1941), pp. 1769ff.

[8] P. von R. Schleyer: J. Am. Chem. Soc. Vol. 79 (1957), pp. 3292ff.

[9] C. A. Cupas, P. von R. Schleyer, and D. J. Trecker: J. Am. Chem. Soc. Vol. 87 (1965), pp. 917ff.

[10] S. Hala, S. Landa, and V. Hanus: Angew. Chem. Internat. Edit. Vol. 5 (1966), pp. 1045ff.

[11] V. Z. Williams, P. von R. Schleyer, G. J. Gleicher, and L. B. Rodewald: J. Am. Chem. Soc. Vol. 88 (1966), pp. 3862ff.

[12] W. Burns, T. Mitchell, M. McKervey, J. Rooney, G. Ferguson, and P. Roberts: J. Chem. Soc. Chem. Commun. Vol. 21 (1976), pp. 893ff.

[13] P. von R. Schleyer, 1990, My Thirty Years in Hydrocarbon Cages: From Adamantane to Dodecahedrane, in G. A. Olah, *Cage Hydrocarbons*, 1-38, John Wiley, New York.

[14] G. P. Moss: Pure Appl. Chem. Vol. 71 (1999), pp. 513ff.

[15] W. Wingert: Fuel Vol. 71 (1992), pp. 37ff.

[16] R. Lin and Z. A. Wilk: Fuel Vol. 74 (1995), pp. 1512ff.

[17] J. E. Dahl, J. M. Moldowan, K. E. Peters, G. E. Claypool, M. A. Rooney, G. E. Michael, M. R. Mello, and M. L. Kohnen: Nature Vol. 399 (1999), pp. 54ff.

[18] Z. Wei, J. M. Moldowan, J. Dahl,T. P. Goldstein and D. M. Jarvie: Org. Geochem. Vol. 37 (2006), pp. 1421ff.

[19] P. Badziag, W. S. Verwoerd, W. P. Ellis and N. R. Greiner: Nature Vol. 343 (1990), pp. 244ff.

[20] J. E. P. Dahl, J. M. Moldowan, T. M. Peakman, J. C. Clardy, E. Lobkovsky, M. M. Olmstead, P. W. May, T. J. Davis, J. W. Steeds, K. E. Peters, A. Pepper, A. Ekuan, and R. M. K. Carlson: Angew. Chem. Int. Ed. Vol. 42 (2003), pp. 2040ff.

[21] M. Z. Shen, H. F. Schaefer, C. X. Liang, J. H. Lii, N. L. Allinger, and P. on R. Schleyer: J. Am. Chem. Soc. Vol. 114 (1992), pp. 497ff.

[22] T. Jefferson, V. Demicheli, C. Di Pietrantonj, and D. Rivetti: Cochrane Database of Systematic Reviews Vol. 2 (2006), CD001169

[23] R. Inzelberg, U. Bonuccelli, E. Schechtman, A. Miniowich, R. Strugatsky, R. Ceravolo, C. Logi, C. Rossi, C. Klein, and J. Martin Rabey: Movement Disorders Vol. 21 (2006), pp. 1375ff.

[24] D. M. Robinson and G. M. Keating: Drugs Vol. 66 (2006), pp. 1515ff.

[25] J.L. Vennerstrom, S. Arbe-Barnes, R. Brun, S.A. Charman, F.C.K. Chiu, J. Chollet, Y. Dong, A. Dorn, D. Hunziker, H. Matile, K. McIntosh, M. Padmanilayam, J.S. Tomas, C. Schuerer, B. Scorneaux, Y. Tang, H. Urwyler, S. Wittlin, and W.N. Charman: Nature Vol. 430 (2004), pp. 900ff.

[26] T. G. Archibald, A. A. Malik, and K. Baum, and M. R. Unroe: Macromolecules Vol. 24 (1991), pp. 5261ff.

[27] K. S. Burnham, R. Roth, F. Zhou, W. Fan, E. Brouk, and M. Stifanos: J. Poly. Sci. A Vol. 44 (2006), pp. 6909ff.

[28] Y-T. Chern and W-H. Chung: Macromol. Chem. Phys. Vol. 197 (1996), pp. 1171ff.

[29] S. Zheng, J. Shi, and R. Mateu: Chem. Mater. Vol. 12 (2000), pp. 1814ff.

[30] H. Y. Jeong, Y. K. Lee , A. Talaie , K.M. Kim, Y.D. Kwon, Y.R. Jang, K.H. Yoo, D.J. Choo, and J. Jang: Thin Solid Films Vol. 417 (2002), pp. 171ff.

[31] S. T. Lee, H. Y. Peng, X. T. Zhou, N. Wang, C. S. Lee, I. Bello, and Y. Lifshitz: Science Vol. 287 (2000), pp. 104ff.

[32] H. Makita, K. Nishimura , N. Jiang, A, Hatta, T. Ito, and A. Hiraki: Thin Solid Films Vol. 282 (1996), pp. 279ff.

[33] G. C. McIntosh, M. Yoon, S. Berber, and D. Tomanek: Phys. Rev. B. Vol. 70 (2004), pp. 045401ff.

[34] G. I. Leacht and R. C. Merkle: Nanotechnology Vol 5. (1994), pp. 168ff.

[35] R. Bailey: Spectrochim. Acta A 27 (1971), pp. 1447ff.

[36] Y.-R. Chen, H.-C. Chang, C.-L. Cheng, C.-C. Wang and J. C. Jiang: J. Chem. Phys. Vol. 119 (2003), pp. 10626ff.

[37] J. Filik, J.N. Harvey, N.L. Allan, P.W. May, J.E.P. Dahl, S. Liu, and R.M.K. Carlson: Phys. Rev. B Vol. 74 (2006), pp. 035423ff.

[38] L. Bistricic, G. Baranovi, and K. Mlinaric-Majerski: Spectrochim. Acta A Vol. 51 (1995), pp. 1643ff.

[39] J. O. Jensen: Spectrochim. Acta A Vol. 60 (2004), pp. 1895ff.

[40] L. Bistricic, G. Baranovic, and K. Mlinaric-Majerski: J. Mol. Struct. Vol. 508 (1999), pp. 207ff.

[41] L. Bistricic, L. Pejov, and G. Baranovic: J. Mol. Struct. Theochem. Vol. 594 (2002), pp. 79ff.

[42] A. Kovacs and A. Szabo: J. Mol. Struct. Vol. 519 (2000), pp. 13ff.

[43] L. Rivas, S. Sanchez-Cortes, J. Stanicova, J. V. Garcia-Ramos, and P. Miskovsky: Vib. Spectrosc. Vol. 20 (1999), pp. 179ff.

[44] T. E. Jenkins and J. Lewis: Spectrochim. Acta A Vol. 36 (1980), pp. 259ff.

[45] S. L. Richardson, T. Baruah, M. J. Mehl, and M. R. Pederson: Chem. Phys. Lett. Vol. 403 (2005), pp. 83ff.

[46] J. Filik, J. Harvey, N. Allan, P. May, J. Dahl, S. Liu, and R. Carlson: Spectrochim. Acta A Vol. 64 (2006), pp. 681ff.

[47] S. A. Solin and A. K. Ramdas: Phys. Rev. B. Vol. 1 (1970), pp. 1687ff.

[48] F. Tuinstra and J. L. Koenig: J. Chem. Phys. Vol. 53 (1970), pp. 1126ff.

[49] A. M. Rao, E. Richter, S. Bandow, B. Chase, P. C. Eklund, K.A. Williams, S. Fang, K. R. Subbaswamy, M. Menon, A. Thess, R.E Smalley, G. Dresselhaus, and M. S. Dresselhaus: Science Vol. 275 (1997), pp. 187ff.

[50] A. C. Ferrari and J. Robertson: Phys. Rev. B Vol. 61 (2000), pp. 14095ff.

[51] M. Yoshikawa, Y. Mori, M. Maegawa, G. Katagiri, H. Ishida, and A.Ishitani: Appl. Phys. Lett. Vol. 62 (1993), pp. 3114ff.

[52] S. Prawer and R. J. Nemanich: Phil. Trans. R. Soc. Lond. A Vol. 362 (2004), pp. 2537ff.

[53] R. J. Nemanich, J. T. Glass, G. Lucovsky, and R. E. Shroder: J. Vac. Sci. Tech. A. Vol. 6 (1988), pp. 1783ff.

[54] R. Pfeiffer, H. Kuzmany, N. Salk, and B. Gunther: Appl. Phys. Lett. Vol. 82 (2003), pp. 4149ff.

[55] A. C. Ferrari and J. Robertson: Phys. Rev. B Vol. 63 (2001), pp. 121405ff.

[56] A. C. Ferrari and J. Robertson: Phil. Trans. R. Soc. Lond. A Vol. 362 (2004), pp. 2477ff.

[57] S. Prawer, K. W. Nugent, D. N. Jamieson, J. O. Orwa, L. A. Bursill, and J. L. Peng: Chem. Phys. Lett. Vol. 332 (2000), pp. 93ff.

[58] P. W. May, S. H. Ashworth, C. D. O. Pickard, M. N. R. Ashfold, T. Peakman and J. W. Steeds: Phys. Chem. Comm. Vol. 1 (1998), paper 4.

[59] D. J. Zhang and R. Q. Zhang: J. Phys. Chem. B Vol. 109 (2005), pp. 9006ff.

[60] R. M. Corn, V. L. Shannon, R. G. Snyder, and H. L. Strauss: J. Chem. Phys. 81 (1984), pp. 5231ff.

[61] O. Guillois, G. Ledoux, and C. Reynaud: Astrophys. J. Vol. 521 (1999), pp. L133ff.

[62] A. J. Lu, B. C. Pan, and J. G. Han: Phys. Rev. B. Vol. 72 (2005), pp. 035447ff.

[63] J. Oomens, N. Polfer, O. Pirali, Y. Ueno, R. Maboudian, P. W. May, J. Filik, J. E. Dahl, S. Liu, and R. M. K. Carlson: J. Mol. Spectrosc. Vol. 238 (2006), pp. 158ff.

[64] T. van Buuren, L. N. Dinh, L. L. Chase, W. J. Siekhaus, and L. J.Terminello: Phys. Rev. Lett. Vol. 80 (1998), pp. 3803ff.

[65] C. Bostedt, T. van Buuren, T. M. Willey, N. Franco, L. J. Terminello, C. Heske, and T. Moller: Appl. Phys. Lett. Vol. 84 (2004), pp. 4056ff.

[66] Y. K. Chang, H. H. Hsieh, W. F. Pong, M.-H. Tsai, F. Z. Chien, P. K. Tseng, L. C. Chen, T. Y. Wang, K. H. Chen, D. M. Bhusari, J. R. Yang, and S. T. Lin: Phys. Rev. Lett. Vol. 82 (1999), pp. 5377ff.

[67] L. Ley, J. Ristein, and R. Graupner: Phys. Rev. Lett. Vol. 84 (2000), pp. 5679ff.

[68] W. F. Pong, M.-H. Tsai, and Y. K. Chang: Phys. Rev. Lett. Vol. 84 (2000), pp. 5680ff.

[69] J-Y. Raty, G. Galli, C. Bostedt, T. W. van Buuren, and L. J. Terminello: Phys. Rev. Lett. Vol. 90 (2003), pp. 037401ff.

[70] N. D. Drummond, A. J. Williamson, R. J. Needs, and G. Galli: Phys. Rev. Lett. Vol. 95 (2005), pp. 096801ff.

[71] A. J. Lu, B. C. Pan, and J. G. Han: Phys. Rev. B Vol. 72 (2005), pp. 035447ff.

[72] T. M. Willey, C. Bostedt, T. van Buuren, J. E. Dahl, S. G. Liu, R. M. K. Carlson, L. J. Terminello, and T. Moller: Phys. Rev. Lett. Vol. 95 (2005), pp. 113401ff.

[73] T. M. Willey, C. Bostedt, T. van Buuren, J. E. Dahl, S. G. Liu, R. M. K. Carlson, R. W. Meulenberg, E. J. Nelson, and L. J. Terminello: Phys. Rev. B Vol. 74 (2006), pp. 205432ff.

[74] A. A. Fokin, B. A. Tkachenko, P. A. Gunchenko, D. V. Gusev, and P. R. Schreiner: Chem. Eur. J. Vol. 11 (2005), pp. 7091ff.

[75] P. R. Schreiner, N. A. Fokina, B. A. Tkachenko, H. Hausmann, M. Serafin, J. E. P. Dahl, S. Liu, R. M. K. Carlson, and A. A. Fokin: J. Org. Chem. Vol. 71 (2006), pp. 6709ff.

[76] B. A. Tkachenko, N. A. Fokina, L. V. Chernish, J. E. P. Dahl, S. Liu, R. M. K. Carlson, A. A. Fokin, and Peter R. Schreiner: Org. Lett. Vol. 8 (2006), pp. 1767ff.

[77] A. A. Fokin, P. R. Schreiner, N. A. Fokina, B. A. Tkachenko, H. Hausmann, M. Serafin, J. E. P. Dahl, S. Liu, and R. M. K. Carlson: J. Org. Chem. Vol. 71 (2006), pp. 8532ff.